JOC The Journal of Organic Chemistry

Article

pubs.acs.org/joc

Chloroform as a Hydrogen Atom Donor in Barton Reductive Decarboxylation Reactions

Junming Ho,[†] Jingjing Zheng,[‡] Rubén Meana-Pañeda,[‡] Donald G. Truhlar,*[,‡] Eun Jung Ko,[§] G. Paul Savage,*[,∥] Craig M. Williams,*[,§] Michelle L. Coote,*[,†] and John Tsanaktsidis*[,∥]

[†]ARC Centre of Excellence for Free-Radical Chemistry and Biotechnology, Research School of Chemistry, Australian National University, Canberra, ACT, Australia

[‡]Department of Chemistry, Supercomputing Institute, and Chemical Theory Center, University of Minnesota, Minneapolis, Minnesota 55455-0431, United States

[§]School of Chemistry and Molecular Biosciences, University of Queensland, Brisbane 4072, Queensland, Australia

[∥]CSIRO Materials Science and Engineering, Clayton South, 3169 Victoria, Australia

Supporting Information

ABSTRACT: The utility of chloroform as both a solvent and a hydrogen atom donor in Barton reductive decarboxylation of a range of carboxylic acids was recently demonstrated (Ko, E. J. et al. *Org. Lett.* **2011**, *13*, 1944). In the present work, a combination of electronic structure calculations, direct dynamics calculations, and experimental studies was carried out to investigate how chloroform acts as a hydrogen atom donor in Barton reductive decarboxylations and to determine the scope of this process. The results from this study show that hydrogen atom transfer from chloroform occurs directly under kinetic control and is aided by a combination of polar effects and quantum mechanical tunneling. Chloroform acts as an effective hydrogen atom donor for primary, secondary, and tertiary alkyl radicals, although significant chlorination was also observed with unstrained tertiary carboxylic acids.

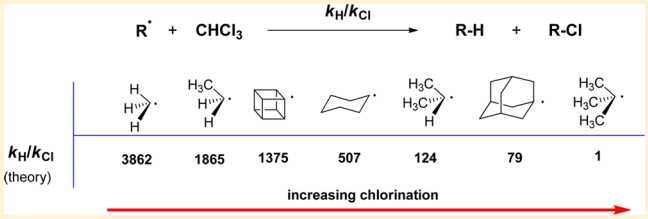

INTRODUCTION

Protodecarboxylation of a carboxylic acid **1** is a fundamental functional group transformation in organic chemistry that formally involves the extrusion of a molecule of carbon dioxide (CO_2) from a carboxylic acid residue, furnishing the corresponding hydrocarbon **2**.[1] While the R-group can in principle be any organic moiety, including alkyl, vinyl, alkynyl, and aryl, only carboxylic acids that contain a neighboring stabilizing group, such as a β-keto group, are capable of undergoing decarboxylation under moderate reaction conditions (Scheme 1).[2]

Protodecarboxylations of alkyl carboxylic acids (**1**, R = alkyl) through the Barton radical decarboxylation protocol in the presence of a suitable hydrogen atom donor (H-donor), also referred to as reductive decarboxylations, are an important subset of this synthetically important reaction class.[3−8] Fundamental to the Barton decarboxylation protocol is the alkyl thiohydroxamic ester **3**, also known as the Barton ester, which is readily prepared (*in situ*) from acid chlorides **4** and 1-hydroxypyridine-2(1*H*)-thione sodium salt **5**, or through the prior reaction of carboxylic acids **1** and 1-hydroxypyridine-2(1*H*)-thione **6** in the presence of a dehydrating agent (Scheme 2).[9] Under the influence of visible light and heat, Barton esters **3** undergo rapid homolytic decomposition furnishing the corresponding alkyl acyloxy radicals **7**, which decarboxylate rapidly[10] to produce the corresponding alkyl radicals **8**, and in turn the reduction product **2** upon interception with a suitable H-donor. Alternatively, in the absence of a competitive H-donor the radical **8** can react with the Barton ester **3** to produce the 2-pyridylsulfide **9**, a process known as self-trapping.

Effective H-donors are typically characterized by a relatively low H-donor bond dissociation enthalpy (BDE), and they give rise to stabilized conjugate radicals that can effectively participate in chain propagation, as exemplified by established H-donors such as tributyltin hydride (TBTH),[11] thiophenol (TP),[12] tris(trimethylsilyl)silane (TTMS),[11] and *tert*-butylthiol (TBT).[13−15] Table 1 lists the best available BDEs and hydrogen atom transfer (HAT) rate constants for these benchmark H-

Scheme 1. Protodecarboxylation of Carboxylic Acids

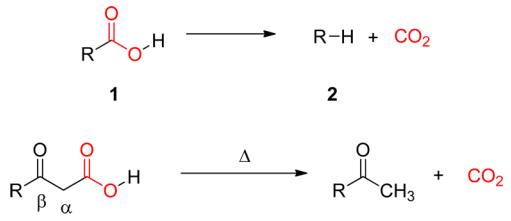

Received: May 8, 2013
Published: June 3, 2013

dx.doi.org/10.1021/jo400927y | J. Org. Chem. 2013, 78, 6677−6687

Scheme 2. Barton Reductive Decarboxylation Process

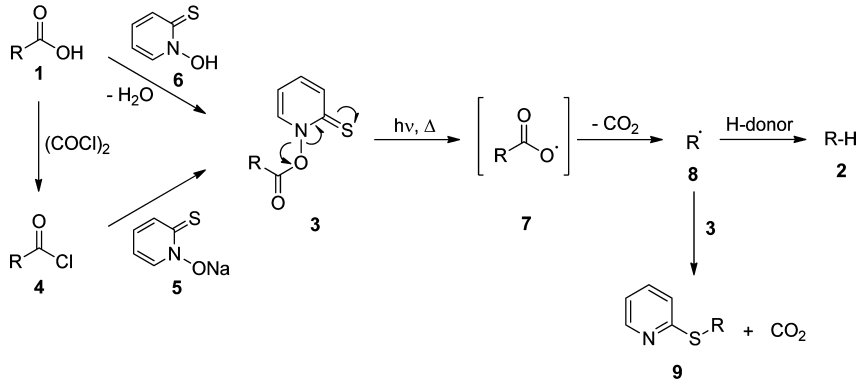

Table 1. Bond Dissociation Enthalpies (BDEs) and Hydrogen Atom Transfer (HAT) Rate Constants with Alkyl Radicals and Some Benchmark H-Donors

H-donor	H-donor BDE (kcal/mol)	HAT rate constants (k_H, M^{-1} s^{-1})[16] for primary alkyl radicals at 25 °C
Bu_3Sn–H	78[11]	2.2×10^6
PhS–H	80[12]	9×10^7
$(Me_3Si)_3Si$–H	84[11]	3.9×10^5
tert-BuS–H	88[13−15]	6×10^6

donors. The use of these H-donors, however, is disadvantaged by their cost, availability, malodorous nature, toxicity, or difficulties associated with product purification. As such, there is an ongoing need for effective H-donors that are inexpensive, readily available, easily handled, and readily removed from the final reaction products.

We have reported recently on chloroform's effectiveness as a H-donor in the Barton reductive decarboxylation reactions of various primary, secondary, and tertiary (including strained bridgehead) alkyl carboxylic acids (Scheme 3).[17] Table 2

Scheme 3. Products Arising from the Homolytic Decomposition of Barton Esters in Chloroform

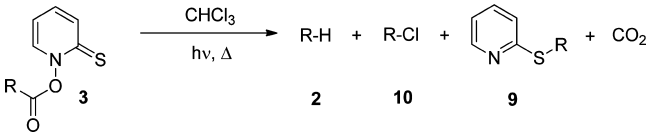

provides a summary of experimental data from both this work and our earlier work that demonstrates this utility. For primary and strained bridgehead carboxylic acids (entries 1−3, 7, and 8) the yields of reduced products **2** are comparable to, if not better than, those obtained using classical H-donor sources such as TBTH and TP. With secondary and tertiary carboxylic acids (entries 4, 5, and 6), however, significant quantities of the corresponding chlorides **10** and the 2-pyridiylsulfides **9** were also produced. This process has since been developed as an *Organic Syntheses* procedure.[18]

While the data presented in Table 2 demonstrate chloroform's hitherto unrecognized synthetic utility as a H-donor, especially for primary and strained bridgehead radicals, it provides little insight into this reactivity, especially when considered through the simple perspective of C–H BDE alone, which for chloroform is 93.8 ± 0.6 kcal mol^{-1}.[19] Simple comparison with the BDEs of H-donors listed in Table 1 highlights the inadequacy of this analysis. Additionally, chlorine atom transfer (CAT) has been shown to be competitive, especially with tertiary alkyl radicals, thereby introducing an added dimension to this observed reactivity of chloroform.

In the present work, we have employed electronic structure and direct dynamics calculations, and additional experimental (including deuterium kinetic isotope effects) studies to examine how chloroform might act as a H-donor in Barton reductive decarboxylation reactions and to better define the scope of the reaction. The results show that HAT from chloroform occurs directly with primary, secondary, and tertiary alkyl radicals under kinetic control and is aided by polar and tunneling effects. With unstrained tertiary carboxylic acids, significant chlorination *via* direct chlorine atom transfer from chloroform is shown to be competitive.

In the next section we describe the methods to compute the Gibbs free energy and the rate constants. Sections 3 and 4 show the results and the discussion respectively.

COMPUTATIONAL METHODS

The thermodynamic data associated with hydrogen and chlorine atom transfer reactions were computed at the G3(MP2)-RAD level of theory[20] in conjunction with MPW1K/6-31+G(d,p) geometries and frequencies. The electronic structure model chemistries were chosen on the basis of a previous assessment study.[21] Scale factors[22] have been applied to the harmonic frequencies in all calculations. To obtain free energies in solution, solvation free energies (at 333 K) were calculated using the SMD[23] model at the M06−2X/6-31+G(d,p)[24] level of theory (which the models were parametrized for) and using chloroform as the solvent on solution phase optimized geometries. The solvation free energies were then combined with the gas phase free energies, taking into account the appropriate standard state corrections, to arrive at the solution phase reaction barriers and free energies with a standard state of 1 mol L^{-1}. The SMD model has been parametrized to predict solvation free energies at 298 K, and we have assumed that the solvation contributions to the reaction and activation Gibbs free energies are the same at 298 and 333 K.

The reaction rate constants for hydrogen and chlorine atom transfer were based on the following rate law: $R = k_{H/Cl}[CHCl_3][R^\bullet]$, where the rate constants $k_{H/Cl}$ were evaluated using variational transition state theory with multidimensional tunneling (VTST/MT).[25] The variational effects were incorporated by canonical variational transition-state theory (CVT), in which the flux is minimized for a canonical ensemble. Tunneling was incorporated using the microcanonically optimized multidimensional tunneling (μOMT) method,[26] which optimizes microcanonically (at every energy) the largest probability between the small curvature tunneling (SCT) probability[27,28] and the large curvature tunneling (LCT) probability,[29] the latter evaluated with the LCG4[29] version of multi-dimensional large curvature

dx.doi.org/10.1021/jo400927y | J. Org. Chem. 2013, 78, 6677−6687

Table 2. Examples of Barton Reductive Decarboxylations in Chloroform[a]

Entry	R-CO_2H **1**	R-H **2** Yield (%)[b]	R-Cl **10** Yield (%)[c]	2-Pyridylsulfide **9** Yield (%)[c]
1[a]	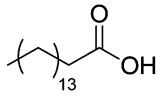 **1a**	 **2a** (86)	**10a** <1	**9a** < 1
2[a]	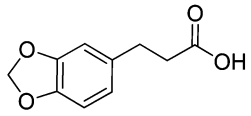 **1b**	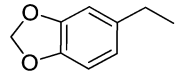 **2b** (77)	**10b** < 1	**9b** 4
3[a]	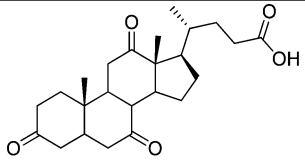 **1c**	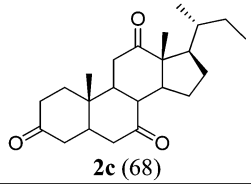 **2c** (68)	**10c** < 1	**9c** < 1
4	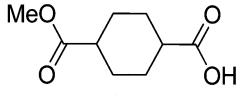 **1d**	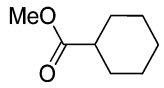 **2d** (77)	**10d** 5	**9d** 3
5	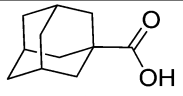 **1e**	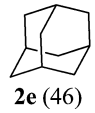 **2e** (46)	**10e** 23	**9e** 11
6	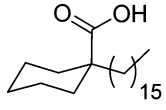 **1f**	 **2f** (48)	**10f** 24	**9f** 6
7	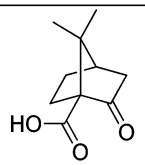 **1g**	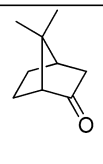 **2g** (86)	**10g** < 1	**9g** < 1
8[a]	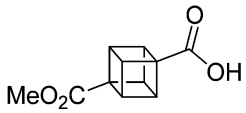 **1h**	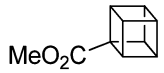 **2h** (82)	**10h** < 1	**9h** < 1

[a]Data taken from ref 17. [b]Isolated yields. [c]Identified and quantified by ^{1}H NMR and/or GCMS where yields were small (<1).

tunneling, interpolated in two dimensions.[30] A detailed description of these procedures is provided in the Supporting Information.

All of the dynamics calculations were computed using the direct dynamics method where all the electronic structure calculations were performed using M06−2X[24] including the solvation effects of the chloroform by the SMD[23] continuum solvation model. The basis set used was 6-31+G(d,p) except for the larger radicals, i.e. cyclohexyl, adamantyl, and cubyl, where the smaller 6-31G(d) basis set was used instead. The MEP was followed in nonredundant curvilinear (internal) coordinates by using the Page−McIver[31] algorithm, and the RODS[32] algorithm was used to maximize the value of the vibrationally adiabatic potential at each point along the MEP optimizing the orientation of the dividing surface. A converged MEP was obtained with a step size of 0.005 Å, scale mass μ = 1 amu, and Hessian calculations every nine steps. All frequencies were scaled by a factor of 0.967 when the 6-31+G(d,p) is used and a factor of 0.963 where the 6-31G(d) is used.[33] All the rate constants have been computed taking into account that the symmetry number is three with the exception of the chlorine atom transfer reaction by the methyl radical where it is nine.[34]

All electronic structure calculations were performed using the *Gaussian 09*[35] and *Molpro* 2009.1[36] programs and the rate constants were computed with the program *GAUSSRATE*,[37] which is an interface between *POLYRATE*[37] and *Gaussian09*.

RESULTS

To understand the role played by the chloroform in Barton reductive decarboxylation, we studied the hydrogen atom transfer (HAT), deuterium atom transfer (DAT), and chlorine atom transfer (CAT) reactions between chloroform and different radicals. That includes methyl and ethyl as primary radicals; isopropyl and cyclohexyl as secondary radicals; and *tert*-butyl and adamantyl as tertiary radicals and cubyl as a tertiary strained bridgehead radical. It should be noted that cyclohexyl and adamantyl radicals are models of the

dx.doi.org/10.1021/jo400927y | J. Org. Chem. 2013, 78, 6677−6687

Table 3. Computed Standard-State Gibbs Free Energies of Activation (in kcal·mol^{-1}) at the Generalized Transition State and Gibbs Free Energies of Reaction (in kcal·mol^{-1}) for the Hydrogen Atom and Chlorine Atom Transfer Reaction between Chloroform and Various Alkyl Radicals at 333 K in Chloroform Solution[a]

R$^\bullet$	$\Delta G_H^{\ddagger,CVT,o}$[b,c]	$\Delta G_{Cl}^{\ddagger,CVT,o}$[b,c]	ΔG_H[d]	ΔG_{Cl}[d]
methyl	14.48 (13.86)	19.47 (19.33)	−7.86 (−8.49)	−10.71 (−11.04)
ethyl	15.31 (14.44)	19.59 (19.42)	−3.26 (−3.94)	−9.51 (−11.22)
isopropyl	15.93 (15.27)	18.61 (18.46)	−0.32 (−0.72)	−10.15 (−10.86)
tert-butyl	16.23 (15.82)	15.94 (15.81)	0.86 (1.43)	−10.34 (−10.65)
cyclohexyl	14.02 (12.95)	17.18 (17.07)	−0.91 (−1.25)	−12.19 (−12.20)
adamantyl	10.68 (10.24)	13.17 (13.13)	−3.25 (−2.17)	−16.59 (−16.09)
cubyl	9.51 (9.31)	14.14 (14.09)	−8.30 (−7.61)	−18.84 (−18.50)
2-pyridinethiol	20.90 (20.78)		8.89	

[a]The standard-state concentration is taken as 1 M. [b]Values in parentheses correspond to the phenomenological free energy of activation, which includes both variational and tunneling effects (i.e., $\Delta G_{phen} = \Delta G^{\ddagger,CVT,o} - RT \ln \kappa$). [c]Computed at the M06−2X/6-31+G(d,p) level of theory using the SMD continuum solvation model. For the cyclohexyl, adamantyl, and cubyl radicals, the 6-31G(d) basis set was used instead. [d]Computed using G3(MP2)-RAD model chemistry in conjunction with solvation free energies from the SMD solvent model. Values in parentheses were computed by M06−2X/6-31+G(d,p) using the SMD continuum solvation model. The results are in very good agreement with G3(MP2)-RAD; therefore the former was used in the direct dynamics calculations for reasons of cost.

Table 4. Computed VTST/μOMT Rate Constants (in M^{-1} s^{-1}) and Barrier Heights (in kcal·mol^{-1}) for the Hydrogen Atom and Chlorine Atom Transfer Reaction between Chloroform and Various Alkyl Radicals at 333 K in Chloroform Solution

R$^\bullet$	k_H	k_D	k_{Cl}	$\Delta V^{\ddagger}$(HAT)[a]	$\Delta V^{\ddagger}$(CAT)[a]
methyl	5.72×10^3	3.31×10^3	1.48×10^0	7.31	10.39
ethyl	2.40×10^3	5.08×10^2	1.29×10^0	7.81	9.16
isopropyl	6.81×10^2	8.25×10^2	5.50×10^0	8.01	8.02
tert-butyl	2.98×10^2	1.73×10^2	3.04×10^2	7.59	6.81
cyclohexyl	2.29×10^4	5.72×10^3	4.52×10^1	6.79	6.89
adamantyl	1.37×10^6	3.34×10^5	1.74×10^4	4.71	4.11
cubyl	5.55×10^6	1.55×10^6	4.03×10^3	4.07	5.66
2-pyridinethiol	1.64×10^{-1}			15.07	

[a]$\Delta V^{\ddagger}$ is the barrier height in the vibrationally adiabatic potential (V_a^G); see eq 5 in the Supporting Information.

experimentally studied systems, 4-carbomethoxycyclohexyl, 4-carbomethoxycubyl respectively. The competing HAT reaction between 2-pyridinethiol and chloroform is also examined. Table 3 shows the Gibbs free energy of activation and reaction for HAT and CAT for various systems at 333 K, where the effect of chloroform as solvent was included. The rate constants for all the reactions described before computed with VTST/μOMT in solution are shown in Table 4, while Table 5 lists the μOMT transmission coefficients. For all of the studied reactions, we found that the differences between μOMT and SCT transmission coefficients are very small (see Supporting Information).

Table 5. Microcanonical Optimized Multidimensional Tunneling (μOMT) Transmission Coefficients for HAT, DAT, and CAT between Chloroform and Various Alkyl Radicals at 333 K in Chloroform Solution

R$^\bullet$	HAT	DAT	CAT
methyl	2.55	3.92	1.25
ethyl	3.77	4.10	1.29
isopropyl	2.71	2.54	1.25
tert-butyl	1.86	1.49	1.22
cyclohexyl	5.08	4.02	1.19
adamantyl	1.96	2.50	1.07
cubyl	1.35	2.09	1.08
2-pyridinethiol	1.20		

DISCUSSION

Direct versus Indirect HAT. Mechanistically, the first event in the Barton reductive decarboxylation process involves the homolytic decomposition of the thiohydroxamic ester **3** to generate the alkyl acyloxy radical **7** and the 2-pyridinethiyl radical **11** (Scheme 4). The acyloxy radical **7** then undergoes rapid decarboxylation[10] to generate the corresponding alkyl radical **8** and CO_2. Pathway A invokes direct HAT from chloroform to the alkyl radical **8**, producing the reduction product **2** and the trichloromethyl radical **12**, which in turn can

Scheme 4. Possible HAT (Pathways A and B) and Propagation Pathways for the Barton Reductive Decarboxylation Reaction with Chloroform as the H-Donor

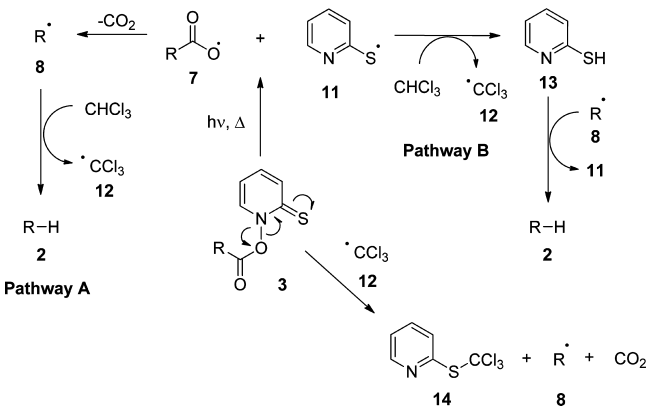

dx.doi.org/10.1021/jo400927y | J. Org. Chem. 2013, 78, 6677−6687

function as a chain carrier by reaction with the thiohydroxamic ester **3**, thereby furnishing trichloromethyl sulfide **14** and a new alkyl radical **8**. Another mechanistic possibility leading to the same overall outcome (Pathway B) requires a rapid HAT from chloroform to the connate 2-pyridinethiyl radical **11**, generating 2-pyridinethiol **13** and **12**. The pyridinethiol **13** would then be expected to react rapidly with **8** to furnish the reduction product **2**, and regenerate **11**, consistent with the well-known ability of thiophenol to function as an effective H-donor to alkyl radicals.[38]

In order to probe the involvement of 2-pyridinethiyl radical **11** in these processes (Pathway B), the reaction of 2,2′-dipyridyl disulfide **15** and chloroform under various reaction conditions was investigated. The participation of **11** in these reactions would be expected to lead to the production of the trichloromethyl sulfide **14** which is a stable, isolable compound (Scheme 5).[39] Irradiation of **15** with a tungsten lamp in

Scheme 5. Reactions of 2,2′-Dipyridyl Disulfide (15) with Chloroform

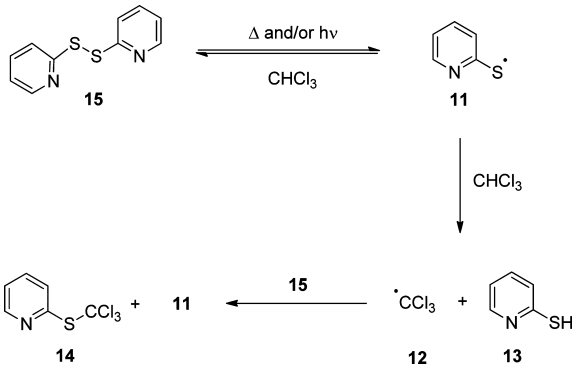

chloroform, and under reflux for several hours, however, did not produce any observable 2-pyridylsulfide **14**. Similarly, UV irradiation (254 nm)[40] of a solution of **15** in chloroform using a Rayonet Reactor at room temperature for 30 min provided no evidence of **14**. These experiments show that HAT from chloroform to the 2-pyridinethiyl radical **11** is not occurring under these conditions.

Pathway B was also studied computationally. The HAT reaction between chloroform and 2-pyridinethiyl radical **11** to generate trichloromethyl radical **12** and 2-pyridinethiol **13** in chloroform solution at 60 °C (or 333 K, i.e. the boiling point of chloroform) was found to be 8.9 kcal/mol endothermic and to proceed with a calculated rate constant for HAT of about 0.2 M^{-1} s^{-1} thereby indicating that Pathway B is not likely to be important due to the very slow formation of 2-pyridinethiol **13**.

For comparison, the direct HAT reaction between chloroform and a series of alkyl radicals was also investigated theoretically, as detailed in Tables 3 and 4. The calculations indicate that these reactions are generally exergonic ($\Delta G_H < 0$), occurring with rate constants (k_H) ranging from 10^2 to 10^6 M^{-1} s^{-1} at 333 K. For the *tert*-butyl radical, experimental values for k_H (2.54×10^2 M^{-1} s^{-1}) and k_{Cl} (1.84×10^2 M^{-1} s^{-1}) at 310 K have been determined[41] and are in good agreement with the corresponding calculated values at this temperature of 1.42×10^2 and 1.17×10^2 M^{-1} s^{-1}, respectively. Accordingly, the combination of these experimental and theoretical studies effectively rules out the involvement of 2-pyridinethiyl radical **11** as a catalyst in these reactions (pathway B, Scheme 4). It follows that HAT must take place directly from $CHCl_3$ to the alky radical **8** (pathway A, Scheme 4).

Self-Trapping. In competition with direct HAT from chloroform, however, are two other processes: (i) CAT leading to chlorination and (ii) self-trapping wherein the alkyl radical **8** reacts with the thiohydroxamic ester **3** to generate the corresponding alkyl 2-pyridyl sulfide **9** (Scheme 6).

Scheme 6. Competitive CAT and Self-Trapping Reactions

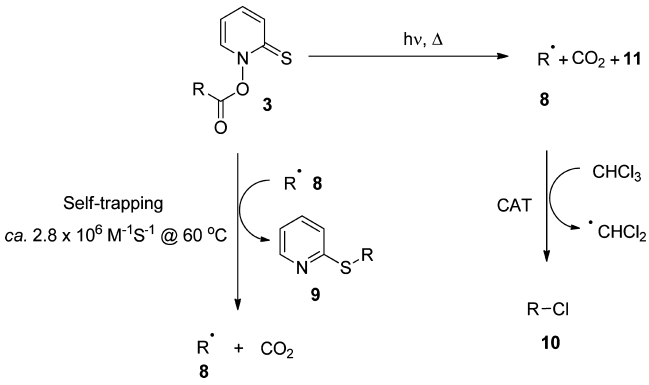

Newcomb and Kaplan have previously determined the rate constant for the reaction of *n*-octyl radical with its precursor thiohydroxamic ester **3** (R = *n*-octyl) to be 2.8×10^6 M^{-1} s^{-1} at 60 °C,[42] which effectively imposes a minimum reactivity for any H-donor to effectively compete with self-trapping. This is the fate of all alkyl thiohydroxamic esters when decomposed homolytically in the absence of a competitive radical trap.[43,44] In the present case the suppression of significant amounts of alkyl 2-pyridyl sulfides **9** can be attributed to the high relative concentration of chloroform ($[CHCl_3]$ = 12.4 M) and the maintenance of a constant but sufficiently low "steady state" *in situ* concentration of thiohydroxamic ester **3**, through the *slow* dropwise addition of the acid chloride **4** to an equivalent of 1-hydroxypyridine-2(1*H*)-thione sodium salt **5** in chloroform. This experimental regimen can be reliably employed to effectively control the relative concentrations of both the thiohydroxamic ester **3** and the alkyl radical **8**, thereby channelling the reaction of the latter toward HAT (and CAT) from chloroform rather than self-trapping with **3** (Schemes 4 and 6).

The only reported rate constant for the abstraction of a hydrogen atom from chloroform by an *n*-alkyl radical comes from the early work of Tuan and Gaumann who studied the radiolysis of liquid binary mixtures of *n*-hexane and chloroform.[45] This study produced a rate constant, k_H, for the HAT from chloroform to *n*-hexyl of 4.8×10^3 M^{-1} s^{-1} at −10 °C. Using the ethyl radical as a model for the *n*-hexyl system, our calculations predict a 9.5-fold increase in rate going from −10 to 60 °C (see Supporting Information). Applying this correction to the −10 °C experimental value yields a k_H of 4.6×10^4 M^{-1} s^{-1} for HAT from chloroform to *n*-hexyl at 60 °C. When combined with the molar concentration of chloroform (12.4 M), an effective rate constant, k_H, of *ca.* 5.7×10^5 M^{-1} s^{-1} is obtained, which becomes competitive with self-trapping (2.8×10^6 M^{-1} s^{-1} at 60 °C). This preference for HAT over self-trapping is further enhanced through controlled low concentrations of thiohydroxamic ester **3**, thereby providing an explanation for the experimental observations.

dx.doi.org/10.1021/jo400927y | J. Org. Chem. 2013, 78, 6677−6687

Chlorine Atom Transfer (CAT) and Polar Effects. As noted in Table 2, significant chlorination (as high as 50% relative to reduction) has been observed in a number of systems, especially with the strain-free tertiary carboxylic acids. To better understand the interplay between HAT and CAT observed in the present work, the thermal rate constants and Gibbs free energies of reaction for the CAT reaction between chloroform and various acyclic and cyclic alkyl radicals were also studied (see Tables 3 and 4 above).

Surprisingly, theoretical calculations predict chlorination to be the thermodynamically preferred pathway ($\Delta G_H - \Delta G_{Cl} \gg 0$), irrespective of the alkyl radical, and predict that this preference increases in progressing from methyl to *tert*-butyl radicals. This is due to a steady decrease in the thermodynamic driving force for HAT, in contrast to the Gibbs reaction energy for CAT (ΔG_{Cl}), which remains relatively constant. For the cyclic radicals there is also a strong thermodynamic preference for CAT over HAT. In contrast to the thermodynamics, the calculated rate coefficients reveal that HAT is faster than CAT for the unstrained radicals and remains competitive with CAT for the strained radicals, despite the overwhelming thermodynamic preference for CAT, mainly because the Gibbs free energies of activation are lower for HAT than for CAT. The collective results thus suggest that the HAT reaction occurs under kinetic control. Clearly, tunneling would favor HAT over CAT; however as discussed in the next section, the size of this effect, though significant, is not sufficient to explain the predominance of the rates of HAT over CAT.

The steady decrease in thermodynamic driving force for HAT is directly related to the increase in radical stability with the increasing degree of alkylation.[46] Accordingly, the contra-thermodynamic behavior of the HAT reactions might indicate that the transition state is early or more reactant-like; however, inspection of the transition state geometries reveals that there is a growing preference for a late transition state for the HAT reaction in the progression from the methyl to *tert*-butyl radical. Shown in Scheme 7 are selected geometrical *ratios* r_1, r_2, r_3, and r_4 which correspond to the ratio of the Cl_3C-H (r_1), R–H (r_2), $H_2ClC-Cl$ (r_3), and R–Cl (r_4) bond lengths (in angstroms) in the HAT and CAT transition states relative to that in the reactants or products. The relative values of r_1 and r_2 and those of r_3 and r_4 provide a measure of the position of the transition state. Accordingly, the steady decrease in r_2 and concurrent increase in r_1 with the increasing degree of alkylation signifies a more product-like transition state as the thermodynamic preference for HAT decreases.

Scheme 7. Ratios of C–H (r_1), R–H (r_2), C–Cl (r_3), and R–Cl (r_4) Bond Lengths (in angstroms) in the HAT and CAT Transition States Relative to That in the Reactants and Products

R•	r_1 r_2 [$Cl_3C\cdots H\cdots R$]‡	r_3 r_4 [$Cl_2HC\cdots Cl\cdots R$]‡
Me•	1.20 1.26	1.14 1.21
Et•	1.23 1.23	1.15 1.21
iPr•	1.26 1.21	1.16 1.21
tBu•	1.28 1.19	1.17 1.20

This raises the question as to why HAT transition states are more stabilized relative to their CAT counterparts. An explanation for the origin of this effect is related to the concept of matched polarities in hydrogen atom transfer reactions[47−49] and may be explained using qualitative concepts from valence bond theory and the curve-crossing model.[50−54] In valence bond theory, the HAT and CAT transition states can be represented as resonance hybrids of the contributing resonance structures depicted in Scheme 8. Since the transition state lies in the part of the reaction coordinate where the reactant and product configurations are of similar energy, the electronic description of the transition state may be described by a resonance hybrid of the two covalent contributors. Additionally, in the HAT reaction, the trichloromethyl radical **12** is also a better electron acceptor (electron affinity = 2.16 eV compared to <0 eV for an alkyl radical).[55] Consequently, an ionic configuration (Cl_3C^- $H^\bullet$ R^+; see Scheme 8) is expected to make a significant contribution to the stability of the transition state, and the size of this resonance effect increases with the electron-donating potential of the alkyl radical. This presumably accounts for the stability of the HAT transition state and explains why the barrier to HAT is relatively insensitive to the stability of the carbon centered radical. This resonance effect is also sometimes referred to as a polar effect[47−49] or charge-shift bonding.[56−58]

In this context, the polar effect is also likely to be more pronounced if the transferring atom is electron withdrawing, as would be the case in CAT from chloroform. This is reflected in the thermodynamics for CAT where the strengthening of the R–Cl bond counteracts the increase in the reactant radical stability as reflected in the nearly constant ΔG_{Cl} in the progression from the methyl to *tert*-butyl radical.[59−61] However, Shaik and co-workers have showed earlier that the ionic contributors associated with a series of halogen transfer identity reactions are accompanied by a significantly higher Pauli repulsion compared to their HAT counterpart.[62] This might explain why the CAT transition states are less stabilized relative to their HAT counterparts. Nonetheless, for strain-free secondary and tertiary alkyl radicals, CAT becomes competitive

Scheme 8. Resonance Contributors for the HAT and CAT Transition States

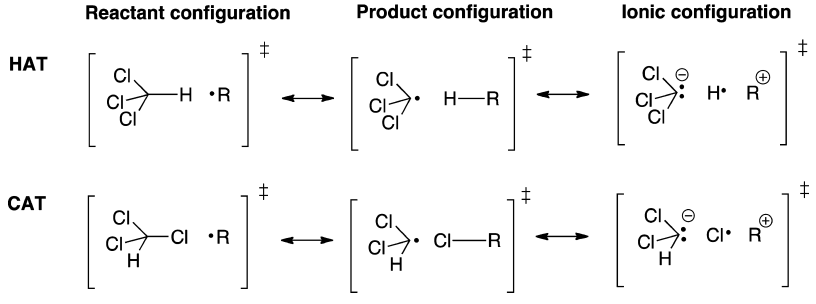

dx.doi.org/10.1021/jo400927y | J. Org. Chem. 2013, 78, 6677−6687

Table 6. Contributions in Ratios of the Rates Constants for HAT, DAT, and CAT Reactions between Chloroform and Various Alkyl Radicals at 333 K in Chloroform Solution

	k_H/k_D				k_H/k_{Cl}				k_D/k_{Cl}			
R•	η_{int}	η_{var}	$\eta_{tun}^{\mu OMT}$	η_{tot}	η_{int}	η_{var}	$\eta_{tun}^{\mu OMT}$	η_{tot}	η_{int}	η_{var}	$\eta_{tun}^{\mu OMT}$	η_{tot}
methyl	5.31	0.50	0.65	1.73	2162.79	0.88	2.04	3861.79	406.98	1.75	3.14	2231.71
ethyl	5.14	1.00	0.92	4.73	642.86	0.99	2.92	1864.49	125.00	0.99	3.17	393.93
isopropyl	0.80	0.96	1.06	0.82	104.24	0.55	2.15	123.77	129.55	0.57	2.02	150.05
tert-butyl	4.95	0.28	1.24	1.72	2.46	0.26	1.52	0.98	0.50	0.94	1.22	0.57
cyclohexyl[a]	5.06	1.01	1.26	6.41	105.20	1.13	4.26	506.67	20.79	1.12	3.38	79.07
adamantyl	5.04	1.04	0.78	4.09	36.00	1.19	1.83	78.55	7.14	1.15	2.35	19.20
cubyl[a]	5.49	1.01	0.65	3.58	1060.75	1.03	1.26	1374.63	193.15	1.02	1.94	383.58

[a]Models of the experimentally studied systems, 4-carbomethoxycyclohexyl, and 4-carbomethoxycubyl respectively.

with HAT as indicated by the experimental product distributions in Table 2 (entries 5 and 6).

Finally, it is also worth noting that the calculated rates of HAT and CAT are higher for cyclic alkyl radicals compared with their acyclic counterparts. For example, the rates of HAT and CAT between chloroform and the cyclohexyl radical are an order of magnitude higher than that of the isopropyl radical. This observation may be understood in terms of the geometry about the radical carbon center in the reactant and the transition state. Carbon-centered radicals generally adopt very near planar geometries whereas their geometry is significantly pyramidal in the transition state. As such, cyclic alkyl radicals are generally strained, and this is manifested in the increased exergonicity and rates of the HAT and CAT reactions, compared to their acyclic analogues as shown in Table 3.

Quantum Mechanical Tunneling. It is well-known that quantum mechanical tunneling effects can play an important role in reactions involving the transfer of light atoms[63] (e.g., hydrogen atom), and this could also directly affect the patterns of reduction versus chlorination observed in the present work. Indeed, earlier work has provided evidence for tunneling effects in hydrogen abstraction reactions between the adamantyl radical and various hydrocarbon solvents.[64−66] Thus, to better delineate the contribution of tunneling in the observed product distributions, the transmission coefficients for HAT and CAT reactions were computed using multidimensional tunneling methods (see Table 5 above), and the ratios of rate coefficients (at 333 K) for HAT versus DAT, HAT versus CAT, and DAT versus CAT are shown in Table 6. The contributions to these ratios (η_{tot}) from classical effects (η_{int}), variational effects ($\eta_{var.}$), and tunnelling ($\eta_{tun}^{\mu OMT}$) are also shown.

The data in Tables 5 and 6 confirm that tunneling typically contributes to a 2-fold increase in the rate of HAT relative to CAT. Even when the classical contribution to the ratio k_H/k_{Cl} is lower than 1, like in the case of the *tert*-butyl radical, tunnelling makes an important contribution to the increase in the HAT rate constant with respect to the CAT rate constant. Indeed for the *tert*-butyl and adamantyl radicals, where the barrier height of the reaction of HAT is higher than the barrier for CAT (see Table 4), tunnelling is greater for the HAT mainly because the mass of the particle that is being transferred is smaller. As shown in Table 6 the ratios are in qualitative agreement with the product branching ratios observed experimentally where chlorination becomes increasingly competitive with reduction from unstrained primary to tertiary radicals.

In light of this, the transfer of a heavier deuterium atom is normally expected to attenuate the effects of tunneling and lead to reductions in the hydrogen (or in this case deuterium) transfer rate, over and above the kinetic isotope effects expected on the basis of vibrational contributions alone. Thus one would expect significant reductions in HAT versus CAT product ratios for the reactions in deuterated chloroform ($CDCl_3$). Although the calculated deuterium atom transfer (DAT) versus CAT ratios presented in Table 6 are consistent with this expectation, this is largely due to quasiclassical kinetic isotope effects rather than tunneling. Indeed, the calculated transmission coefficients for DAT are relatively similar to those for HAT, and actually slightly larger for the smaller alkyl radicals. This effect is unusual but not unprecedented[67−72] and can be explained by noting that the tunneling depends not only on the masses but also on the height and width of the barrier. Indeed, further analysis (see Supporting Information) confirms that the barrier width for DAT is narrower than that for HAT which is the critical factor with regard to determining the transmission coefficient. The larger barrier width associated with HAT is attributed to the higher frequencies associated with the bending modes that involve the transferred atom. For the larger alkyl radicals, the HAT transmission coefficient is higher than that for DAT (consistent with expectation) and this is presumably because the contribution of these bending modes diminishes.

To provide some experimental support for our calculations, we repeated our experiments using $CDCl_3$ but otherwise identical conditions for a representative set of alkyl carboxylic acids and the resulting product ratios are included in Table 7 below. As shown, the rate of deuterium transfer is significantly slower and this generally resulted in an approximately 10-fold reduction in the product ratio of reduction to chlorination, in qualitative agreement with our calculations on *model systems*. Thus, the combined theoretical calculations and experimental results suggest that Barton reductive decarboxylation reaction

Table 7. Experimental k_H/k_{Cl} and k_D/k_{Cl} Determined Using $CHCl_3$ and $CDCl_3$, Respectively

R•	k_H/k_{Cl}[a]	k_H/k_{Cl}[c]	k_D/k_{Cl}[c,d]	k_H/k_D[e]
palmityl	>86[b]	79.4	7.4	10.7
4-carbomethoxycyclohexyl	15	7.8	0.5	15.6
adamantyl	2	0.6	0.1	6
4-carbomethoxycubyl	>82[b]	98	9.4	10.4

[a]Based on data from Table 2. [b]These values represent lower bounds of k_H/k_{Cl} because the yield reported for the reduced product is after purification and thus include losses. [c]This work: H/D to Cl product ratios determined by GC/MS on crude reaction mixtures. [d]The k_D/k_{Cl} ratios are an average of 2 runs. Higher proportions of the corresponding 2-pyridylsulfides (**9a**, **d**, **e**, and **g**) were produced in these reactions, consistent with a slower overall transfer of D. No attempt was made to isolate the products in these reactions. [e]Obtained from data in columns 2 and 3.

dx.doi.org/10.1021/jo400927y | J. Org. Chem. 2013, 78, 6677−6687

occurs under kinetic control predominantly due to favorable polar effects and is aided by quantum mechanical tunneling.

CONCLUSION

We have shown through a combination of mechanistic and theoretical studies that the chloroform-assisted, Barton reductive decarboxylation process involves direct HAT from chloroform to alkyl radicals. Our theoretical calculations predict that, while CAT is the thermodynamically preferred process, HAT proceeds via a lower free energy barrier due to favorable polar effects. These effects, in combination with quantum mechanical tunneling (as confirmed by kinetic isotope studies), confirm that the chloroform-assisted Barton reductive decarboxylation process proceeds under kinetic control.

The present reaction protocol has also been carefully designed to exploit concentration effects to minimize the formation of side products associated with self-trapping. The end result is that the nature of the alkyl radical is critical to the experimental outcome, with primary alkyl and strained bridgehead systems delivering optimal conversions of protodecarboxylation products. CAT becomes competitive for strain-free tertiary alkyl radicals as a result of increased resonance interaction with the ionic configuration.

The collective results highlight the limitations associated with the sole use of BDEs in screening for suitable H-donors, as was also recently noted for the selection of chain carrier agents.[61] It is envisaged that the mechanistic insight developed through this work will provide users of the Barton decarboxylation procedure the ability to design optimized synthetic outcomes. Finally, this process avoids the common toxic or miasmic conditions normally associated with the H-donors (viz. TBTH, TBT, and TP) typically used in Barton reductive decarboxylation reactions and as such should find wide application in both academic and industrial laboratories.

EXPERIMENTAL SECTION

^{1}H and ^{13}C NMR spectra were recorded in deuteriochloroform ($CDCl_3$) unless otherwise stated. Coupling constants are given in Hz, and chemical shifts are expressed as δ values in ppm. Low resolution electrospray ionization mass spectrometry measurements (LRESIMS) were recorded in positive ionization mode using a high capacity 3D ion trap instrument. High resolution electrospray ionization (HRESIMS) accurate mass measurements were recorded in positive mode on a quadrupole−time of flight instrument. Accurate mass measurements were carried out with external calibration using sodium formate as the reference calibrant. H/D to Cl product ratio analyses were undertaken using a GCMS. The GC was coupled to a quadrupole mass spectrometer operating in electron ionization (EI) mode at 70 eV. The GC separation was performed using a fused silica column (30 m × 0.25 mm i.d., 0.25 mm film thickness; 5% phenylmethylpolysiloxane). The oven temperature was programmed as follows: 50 °C (hold 4 min); 10 °C/min to 280 °C (hold 3 min). The total running time was 30 min. Ultrahigh purity helium was used as the carrier gas at a constant flow of 0.7 mL/min. The interface and ion source temperatures were set to 250 and 180 °C, respectively. A solvent delay of 4 min was used to prevent damage in the ion source filament. Column chromatography was undertaken on silica gel (flash silica gel 230−400 mesh), with distilled solvents. Analytical high performance liquid chromatography was performed using a C18 5 μm column. Chloroform and D-chloroform were distilled from a phosphorus pentoxide still and stored over 3A molecular sieves under an atmosphere of nitrogen. Melting points were determined on a melting point apparatus and are uncorrected.

General Method for the Barton Reductive Decarboxylation in Chloroform. To a solution/suspension of the appropriate acid (1 mmol) in chloroform (5 mL) were added oxalyl chloride (94 μL, 1.2 mmol) and one drop of *N,N*-dimethyl formamide, and the reaction was stirred at rt under argon. The formation of the acid chloride was monitored by IR. The crude reaction mixture (Note: excess oxalyl chloride and HCl can be removed prior to addition to the under reduced pressure and the resulting residue redissolved in chloroform) was then added dropwise to a suspension of 1-hydroxypyridine-2(1*H*)-thione, Na salt (179 mg, 1.5 mmol), and 4-*N,N*-dimethylaminopyridine (1 mg, 0.1 mmol) in chloroform (5 mL), with concomitant irradiation from a tungsten lamp (240 V, 500 W). The reaction mixture took on a bright yellow appearance, and CO_2 evolution became evident. After 15 min to 1 h the bright yellow coloration had faded. Heating and irradiation were then discontinued. The reaction mixture was partitioned between CH_2Cl_2 or $CHCl_3$ (20 mL) and 1 N HCl (20 mL), and the organic layer was then further washed with 1 N HCl (2 × 20 mL) and brine (20 mL), dried over $MgSO_4$, and concentrated. Purification by column chromatography (SiO_2) yielded the desired products. For the more volatile substrates, the solvent was removed *in vacuo* from the reaction mixture and the resulting residue partitioned between Et_2O (20 mL) and 1 N HCl (20 mL). The organic layer was then further washed with 1 N HCl (2 × 20 mL) and brine (20 mL), dried over $MgSO_4$, and concentrated. Purification by column chromatography (SiO_2) yielded the desired products.

Pentadecane (2a). Purification by column chromatography (SiO_2, pentane) yielded **2a** (182 mg, 86%) as a colorless oil; ν_{max}/cm^{-1} (film) 2921, 2853, 1465; ^{1}H NMR (400 MHz, $CDCl_3$) δ_H 1.25 (26H, br s), 0.87 (6H, t, J = 6.85 Hz); ^{13}C NMR (100 MHz, $CDCl_3$) δ_C 31.9 (2 × CH_2), 29.7 (5 × CH_2), 29.7 (2 × CH_2), 29.4 (2 × CH_2), 22.7 (2 × CH_2), 14.1 (2 × CH_3); m/z LRMS (EI): 212.4 ([M]$^+$).

5-Ethylbenzo[*d*][1,3]dioxole (2b). Purification by column chromatography (SiO_2, (1:10) Et_2O/Pet) yielded **2b** (116 mg, 77%) as a colorless oil and **9b** (10 mg; 4%) as pale yellow residue.

2b: ν_{max}/cm^{-1} (film) 2965, 2875, 1503, 1486, 1232, 1037; ^{1}H NMR (500 MHz, $CDCl_3$)δ_H 6.73 (1H, d, J = 7.9 Hz), 6.70 (1H, dd, J = 1.7, 0.4 Hz), 6.65 (1H, dd, J = 7.9, 1.7 Hz), 5.92 (2H, s), 2.58 (2H, q, J = 7.6 Hz), 1.20 (2H, t, J = 7.6 Hz); ^{13}C NMR (100 MHz, $CDCl_3$) δ_C 147.5, 145.4, 138.2, 120.4, 108.4, 108.1, 100.7, 28.6, 15.9; m/z LRMS (EI): 150 (50% [M]), 135 (100%).

9b: Collection of HRMS or elemental analysis of this compound was not possible due to its limited stability. ν_{max}/cm^{-1} (film) 2889, 1577, 1501, 1487 1414; ^{1}H NMR (400 MHz, $CDCl_3$) δ_H 8.43 (1H, ddd, J = 4.9, 1.9, 0.9 Hz), 7.44 (1H, ddd, J = 8.0, 7.4, 1.9 Hz), 7.15 (1H, dt, J = 8.0, 0.9 Hz), 6.95 (1H, ddd, J = 7.4, 4.9, 0.9 Hz), 6.76−6.68 (3H, m), 5.91 (2H, s), 3.36 (2H, dd, J = 8.5, 6.9 Hz), 2.91 (2H, dd, J = 8.5, 6.9 Hz); ^{13}C NMR (100 MHz, $CDCl_3$) δ_C 158.8, 149.5, 147.5, 146.0, 135.7, 134.4, 122.3, 121.5, 119.2, 109.1, 108.1, 100.8, 35.5, 31.6; m/z LRMS (ES$^+$): 282.1 (100% [MNa]$^+$); HRMS (ES$^+$): Found [MNa]$^+$ 282.0557, $C_{14}H_{13}NNaO_2S$ requires 282.05779.

24-Norcholane-3,7,12-trione (2c). Purification by column chromatography (SiO_2, (1:2) EtOAc/Petrol) yielded **2c** (243 mg, 68%) as colorless crystals; $[\alpha]_D$ = 14.5 (c = 0.94, $CHCl_3$); mp >250 °C (hexanes); ν_{max}/cm^{-1} (film) 2920, 2868, 1712, 1182; ^{1}H NMR (500 MHz, $CDCl_3$) δ_H 2.91−2.84 (2H, m), 2.82 (1H, t, J = 10.5 Hz), 2.36−1.90 (12H, m), 1.81 (1H, dt, J = 11.3, 7.1 Hz), 1.58 (1H, td, J = 14.4, 4.6 Hz), 1.50−1.40 (1H, m), 1.37 (3H, s), 1.31−1.05 (4H, m), 1.04 (3H, s), 0.83 (3H, t, J = 7.3 Hz), 0.79 (3H, d, J = 6.5 Hz); ^{13}C NMR (100 MHz, $CDCl_3$) δ_C 212.1, 209.1, 208.8, 56.9, 51.8, 49.0, 46.8, 45.6, 45.5, 45.0, 42.8, 38.7, 37.4, 36.5, 36.0, 35.3, 27.8, 27.7, 25.2, 21.9, 18.4, 11.8, 10.8; m/z LRMS (ES$^+$): 381.2 (100% [MNa]$^+$); 298.3 (100%); HRMS (ES$^+$): Found [MNa]$^+$ 381.2388, $C_{23}H_{34}NaO_3$ requires 381.2400.

Methyl Cyclohexanecarboxylate (2d) (2 mmol scale). Purification by column chromatography (SiO_2, (1:10) Et_2O/pentane) yielded **2d** (203 mg, 77%) as a colorless oil, methyl 4-chlorocyclohexanecarboxylate (**10d**) (17 mg, 5%, mixture of diastereoisomers) as a colorless oil, and methyl 4-(pyridin-2-ylthio)cyclohexanecarboxylate (**9d**) (15 mg; 3%, mixture of diastereoisomers) as a pale yellow residue.

2d: ν_{max}/cm^{-1} (film) 2931, 2856, 1732, 1168; ^{1}H NMR (400 MHz, $CDCl_3$) δ_H 3.65 (3H, s), 2.30 (1H, tt, J = 11.3, 3.7 Hz), 1.94−1.84 (2H, m), 1.79−1.69 (2H, m), 1.63 (1H, m), 1.51−1.36 (1H, m),

dx.doi.org/10.1021/jo400927y | J. Org. Chem. 2013, 78, 6677−6687

1.33−1.16 (3H, m); ^{13}C NMR (100 MHz, $CDCl_3$) δ_C 176.6, 51.4, 43.1, 29.0 (2 × CH_2), 25.7, 25.4 (2 × CH_2); *m*/*z* LRMS (ES^+): 165.1 (100% $[MNa]^+$).

10d: ν_{max}/cm^{-1} (film) 2951, 1730, 1436, 1219; ^{1}H NMR (400 MHz, $CDCl_3$) (2:1 mixture of two diastereoisomers) δ_H 4.34−4.25 (1H, m, major), 3.90−3.80 (1H, m, minor), 3.67 (3H, s, major), 3.65 (3H, s, minor), 2.42−2.27 (1H, m, major +1H, m, minor), 2.26−1.48 (8H, m, major +8H, m, minor); ^{13}C NMR (100 MHz, $CDCl_3$) δ_C 175.4, 175.3, 58.5 (2 × CH_2 minor), 58.4 (2 × CH_2 major), 51.7 (2 × CH_2 major, CH_2 minor), 41.4, 35.7, 33.3 (CH_3 major + minor), 29.7, 28.1, 23.7; *m*/*z* LRMS (ES^+): 199.1 (100% $[MNa]^+$).

9d: Collection of HRMS or elemental analysis of this compound was not possible due to its limited stability. ^{1}H NMR (400 MHz, $CDCl_3$) (5:4 mixture of two diastereoisomers) δ_H 8.39 (1H, dddd, *J* = 4.8, 2.7, 1.9, 0.9 Hz, major + minor), 7.43 (1H, dddd, *J* = 8.0, 7.4, 3.5, 1.9 Hz, major + minor), 7.12 (1H, ddt, *J* = 8.0, 3.5, 0.9 Hz, major + minor), 6.93 (1H, dddd, *J* = 7.4, 4.8, 3.5, 0.9 Hz, major + minor), 4.18−4.09 (1H, m, minor), 3.77−3.67 (1H, m, major), 3.66 (3H, s, major), 3.65 (3H, s, minor), 2.43 (2H, tt, *J* = 8.7, 4.2 Hz, major), 2.32 (2H, tt, *J* = 11.9, 3.6 Hz, minor), 2.24−2.17 (2H, m, major), 2.09−1.99 (2H, m, minor), 1.99−1.73 (8H, m, major + minor), 1.68−1.55 (2H, m, major), 1.43 (2H, m, minor); ^{13}C NMR (100 MHz, $CDCl_3$) δ_C 175.9, 175.6, 158.8, 158.7, 149.6, 149.5, 135.9, 135.8, 123.0, 122.9, 119.4, 119.4, 51.6 (2 × CH_3), 42.4, 41.8, 41.4, 41.0, 32.2 (2 × CH_2), 30.3 (2 × CH_2), 29.0 (2 × CH_2), 25.7 (2 × CH_2).

Adamantane (2e). Purification by column chromatography (SiO_2, pentane) yielded **2e** and 1-chloroadamantane (**10e**) as a 2:1 mixture (69% combined yield) as a colorless solid and 2-(adamantan-1-ylthio)pyridine (**9e**) (26 mg, 11%) as a pale yellow residue.

2e: ν_{max}/cm^{-1} (film) 2899, 2848, 1450; ^{1}H NMR (300 MHz, $CDCl_3$) δ_H 1.86 (4H, br s), 1.74 (12H, t, *J* = 3.4 Hz); ^{13}C NMR (75 MHz, $CDCl_3$) δ_C 37.7 (6 × CH_2), 28.3 (4 × CH); *m*/*z* LRMS (EI): 136.3 ($[M]^+$).

10e: ^{1}H NMR (400 MHz, $CDCl_3$) (δ_H 2.12 (9H, br s), 1.66 (6H, br s); ^{13}C NMR (100 MHz, $CDCl_3$) δ_C 68.9, 47.8 (2 × CH_2), 35.6 (4 × CH_2), 31.7 (3 × CH).

9e: ν_{max}/cm^{-1} (film) 2908, 2851, 1575, 1450; ^{1}H NMR (300 MHz, $CDCl_3$) δ_H 8.51 (1H, ddd, *J* = 4.9, 2.0, 0.9 Hz), 7.54−7.48 (1H, m), 7.36 (1H, dt, *J* = 7.6, 1.0 Hz), 7.09 (1H, ddd, *J* = 7.6, 4.9, 1.0 Hz), 2.06 (6H, br d, *J* = 2.9 Hz), 2.02 (3H, br s), 1.67 (6H, t, *J* = 3.0 Hz); ^{13}C NMR (100 MHz, $CDCl_3$) δ_C 156.8, 149.6, 136.0, 129.0, 121.3, 50.0, 43.6 (2 × CH_2), 36.3 (4 × CH_2), 30.1 (3 × CH); *m*/*z* LRMS (ES^+): 246.1 (100% $[MH]^+$); HRMS (ES^+): Found $[MH]^+$ 246.1318, $C_{15}H_{20}NS$ requires 246.1311.

Hexadecylcyclohexane (2f). Purification by column chromatography (SiO_2, petrol) yielded **2f** and 1-chloro-1-hexadecylcyclohexane (**10f**) as a 2:1 mixture (72% combined yield) as a colorless oil, and further elution (10:1 petrol/Et_2O) yielded 2-((1-hexadecylcyclohexyl)-thio)pyridine (**9f**) (25 mg, 6%) as a pale yellow residue.

2f: ν_{max}/cm^{-1} (film) 2920, 2851, 1449; ^{1}H NMR (400 MHz, $CDCl_3$) δ_H 1.72−1.58 (3 H, m), 1.33−1.04 (38H, m), 0.86 (3H, t, *J* = 6.9 Hz); ^{13}C NMR (100 MHz, $CDCl_3$) δ_C 37.7, 37.6, 33.5 (2 × CH_2), 31.9, 30.0, 29.7 (8 × CH_2), 29.6, 29.4, 26.9, 26.8, 26.5 (2 × CH_2), 22.7, 14.1; *m*/*z* LRMS (EI): 308.6 (100% [M]).

10f: ν_{max}/cm^{-1} (film) 2922, 2853, 1462; ^{1}H NMR (400 MHz, $CDCl_3$) δ_H 1.92 (2 H, br d, *J* = 14.6 Hz), 1.78−1.58 (5H, m), 1.57−1.42 (6H, m), 1.34−1.08 (27H, m), 0.86 (3H, t, *J* = 6.9 Hz); ^{13}C NMR (100 MHz, $CDCl_3$) δ_C 39.7 (2 × CH_2), 33.5, 31.9, 29.8, 29.7 (8 × CH_2), 29.6, 29.5, 29.4, 25.5, 23.7, 22.7, 22.4 (2 × CH_2), 14.1; *m*/*z* LRMS (EI): 306.6 (100% [M−Cl]).

9f: Collection of HRMS or elemental analysis of this compound was not possible due to its limited stability. ^{1}H NMR (300 MHz, $CDCl_3$) δ_H 8.46 (1H, ddd, *J* = 4.9, 2.0, 1.0 Hz), 7.46 (1H, ddd, *J* = 7.9, 7.4, 2.0 Hz), 7.31 (1H, dt, *J* = 7.9, 1.0 Hz), 7.03 (1H, ddd, *J* = 7.4, 4.9, 1.0 Hz), 2.07−1.92 (2H, m), 1.75−1.38 (34H, m), 1.22 (28H, br d, *J* = 10.3 Hz), 0.86 (3H, t, *J* = 6.7 Hz); ^{13}C NMR (75 MHz, $CDCl_3$) δ_C 158.3, 149.5, 135.8, 128.0, 120.7, 56.5, 36.6 (2 × CH_2), 31.9, 30.0, 29.7−29.6 (10 × CH_2), 29.4, 26.0, 23.7, 22.7, 22.3 (2 × CH_2), 14.1.

7,7-Dimethylbicyclo[2.2.1]heptan-2-one (2g). Purification by column chromatography (SiO_2, petrol) yielded **2g** (119 mg, 86%) as a colorless solid.

2g: ν_{max}/cm^{-1} (film) 2899, 2848, 1450; ^{1}H NMR (400 MHz, $CDCl_3$) δ_H 2.43−2.33 (1H, m), 2.07−1.93 (4H, m), 1.76 (1H, d, *J* = 18.3 Hz), 1.49−1.33 (2H, m), 1.02 (6H, s); ^{13}C NMR (100 MHz, $CDCl_3$) δ_C 218.6, 58.3, 45.4, 44.2, 43.4, 27.6, 22.7, 21.7, 20.7; *m*/*z* LRMS $(ES)^+$: 161.1 ($[MNa]^+$).

Methyl Cubanecarboxylate (2h). Purification by column chromatography (SiO_2, (1:8) Et_2O/Petrol) yielded **2h** (132 mg, 82%) as colorless crystals; mp 51.2−52.9 °C (hexanes) [ref 7; mp 51.8−52.5 °C]; ν_{max}/cm^{-1} (film) 2987, 1722, 1319, 1221; ^{1}H NMR (400 MHz, $CDCl_3$) δ_H 4.27−4.18 (3H, m), 4.04−3.93 (4H, m), 3.67 (3H, s); ^{13}C NMR (100 MHz, $CDCl_3$) δ_C 172.8, 55.7, 51.4, 49.5 (3 × CH), 47.8, 45.2 (3 × CH); *m*/*z* LRMS (ES^+): 185.0 (100% $[MNa]^+$).

General Procedure for Barton Reductive Decarboxylations in Chloroform and D-Chloroform. To a solution/suspension of the appropriate acid (2 mmol) in chloroform (10 mL) were added oxalyl chloride (260 μL, 380 mg, 3 mmol) and one drop of *N*,*N*-dimethylformamide, and the reaction was stirred at rt under nitrogen until gas evolution ceased, then concentrated under reduced pressure using a rotary evaporator (diaphragm pump pressure; bath temperature set to 40 °C), and then released to nitrogen. The crude acid chloride was then dissolved in either dry chloroform or D-chloroform (10 mL) and added dropwise over ∼10 min to a suspension of 1-hydroxypyridine-2(1*H*)-thione, Na salt (450 mg, 3 mmol), and 4-*N*,*N*-dimethylaminopyridine (5 mg, 0.04 mmol) in either dry chloroform or D-chloroform (10 mL), with concomitant irradiation from a tungsten lamp (240 V, 150 W). The reaction mixture took on a bright yellow appearance, and CO_2 evolution became evident. After 1 h of heating and irradiation were discontinued and the reaction mixture cooled to rt, it was diluted with dichloromethane (30 mL), washed with saturated aqueous $NaHCO_3$ solution (50 mL), and dried over $MgSO_4$. This solution was analyzed by by GCMS.

Reaction of 2,2′-Dipyridyl Disulfide 14 with Chloroform under Irradiation and Heating (Pathway B). A solution of 2,2′-dipyridyl disulfide **14** (2.2g, 1 mmol) in chloroform (10 mL) was purged with nitrogen for several minutes and then irradiated (and heated under reflux) with either a tungsten or low pressure Hg vapor lamp (Rayonet Reactor). The progress of the reaction was monitored by TLC. Even after prolonged treatment (10 h), only starting material was present. ^{1}H NMR of the crude sample after simple solvent removal and after aqueous workup showed 2,2′-dipyridyl disulfide **14** with some baseline peaks indicating formation of some degradation products. No loss in mass of starting material recovered after workup occurred.

■ ASSOCIATED CONTENT

Ⓢ Supporting Information

Experimental procedures, discussion of computational results, including Cartesian coordinates of all studied species in gas phase, and ^{1}H and ^{13}C spectra for all isolated compounds listed in Table 2 are provided in the Supporting Information. This material is available free of charge via the Internet at http://pubs.acs.org.

■ AUTHOR INFORMATION

Corresponding Author

*E-mail: John.Tsanaktsidis@csiro.au; mcoote@rsc.anu.edu.au; c.williams3@uq.edu.au; Paul.Savage@csiro.au; truhlar@umn.edu.

Notes

The authors declare no competing financial interest.

■ ACKNOWLEDGMENTS

We thank the Australian National University, CSIRO, and the University of Queensland for financial support. M.L.C.

gratefully acknowledges generous allocations of supercomputing time on the National Facility of the Australian National Computational Infrastructure, support from the Australian Research Council (ARC) under its Centres of Excellence Scheme, and receipt of an ARC Future Fellowship. This work is also supported in part by the National Science Foundation of the U.S.A. C.M.W. gratefully acknowledges generous support from the Australian Research Council (ARC), and receipt of an ARC Future Fellowship.

REFERENCES

(1) Rodríguez, N.; Goossen, L. *Chem. Soc. Rev.* **2011**, *40*, 5030−5048.
(2) Logue, M. W.; Pollack, R. M.; Vitullo, V. P. *J. Am. Chem. Soc.* **1975**, *97*, 6868−6869.
(3) Barton, D. H. R.; Hervé, Y.; Potier, P.; Thierry, J. *J. Chem. Soc., Chem. Commun.* **1984**, 1298−1299.
(4) Barton, D. H. R.; Crich, D.; Motherwell, W. B. *J. Chem. Soc., Chem. Commun.* **1983**, 939−941.
(5) Della, E. W.; Tsanaktsidis, J. *Aust. J. Chem.* **1986**, *39*, 2061−2066.
(6) Eaton, P. E.; Nordari, N.; Tsanaktsidis, J.; Upadhyaya, S. P. *Synthesis* **1995**, *1995*, 501−502.
(7) Yoshimi, Y.; Itou, T.; Hatanaka, M. *Chem. Commun.* **2007**, 5244−5246.
(8) Saraiva, M. c. F.; Couri, M. R. C.; Hyaric, M. L.; Almeida, M. V. d. *Tetrahedron* **2009**, *65*, 3563−3572.
(9) Barton, D. H. R.; Samadi, M. *Tetrahedron* **1992**, *48*, 7083−7090.
(10) Fraind, A.; Turncliff, R.; Fox, T.; Sodano, J.; Ryzhkov, L. R. *J. Phys. Org. Chem.* **2011**, *24*, 809−820.
(11) Laarhoven, L. J.; Mulder, P.; Wayner, D. D. *Acc. Chem. Res.* **1999**, *32*, 342−349.
(12) Zavitsas, A. A.; Chatgilialoglu, C. *J. Am. Chem. Soc.* **1995**, *117*, 10645−10654.
(13) Escoubet, S.; Gastaldi, S.; Vanthuyne, N.; Gil, G.; Siri, D.; Bertrand, M. P. *J. Org. Chem.* **2006**, *71*, 7288−7292.
(14) Henríquez, C.; Bueno, C.; Lissi, E. A.; Encinas, M. V. *Polymer* **2003**, *44*, 5559−5561..
(15) Maung, N. *THEOCHEM* **1999**, *460*, 159−166.
(16) Jin, J.; Newcomb, M. *J. Org. Chem.* **2007**, *72*, 5098−5103.
(17) Ko, E. J.; Savage, G. P.; Williams, C. M.; Tsanaktsidis, J. *Org. Lett.* **2011**, *13*, 1944−1947.
(18) Ko, E. J.; Williams, C. M.; Savage, G. P.; Tsanaktsidis, J. *Org. Synth.* **2012**, *89*, 471−479.
(19) Luo, Y.-R. *Handbook of bond dissociation energies in organic compounds*; CRC Press: 2007.
(20) Henry, D. J.; Sullivan, M. B.; Radom, L. *J. Chem. Phys.* **2003**, *118*, 4849−4860.
(21) Beare, K. D.; Coote, M. L. *J. Phys. Chem. A* **2004**, *108*, 7211−7221.
(22) Merrick, J. P.; Moran, D.; Radom, L. *J. Phys. Chem. A* **2007**, *111*, 11683−11700.
(23) Marenich, A. V.; Cramer, C. J.; Truhlar, D. G. *J. Phys. Chem. B* **2009**, *113*, 6378−6396.
(24) Zhao, Y.; Truhlar, D. G. *Theor. Chem. Acc.* **2008**, *120*, 215−241.
(25) Fernandez-Ramos, A.; Ellingson, B. A.; Garrett, B. C.; Truhlar, D. G. In *Reviews in Computational Chemistry*; Lipkowitz, K. B., Cundari, T. R., Eds.; Wiley-VCH: Hoboken, NJ, pp 125−232, 2007; Vol. *23*.
(26) Liu, Y.-P.; Lynch, G. C.; Truong, T. N.; Lu, D.-h.; Truhlar, D. G. *J. Am. Chem. Soc.* **1993**, *115*, 2408−2415.
(27) Skodje, R. T.; Truhlar, D. G.; Garrett, B. C. *J. Phys. Chem.* **1981**, *85*, 3019−3023.
(28) Liu, Y.-P.; Lu, D.-h.; González-Lafont, A.; Truhlar, D. G.; Garrett, B. C. *J. Am. Chem. Soc.* **1993**, *115*, 7806−7817.
(29) Fernandez-Ramos, A.; Truhlar, D. G. *J. Chem. Phys.* **2001**, *114*, 1491−1496.
(30) Fernandez-Ramos, A.; Truhlar, D. G. *J. Chem. Theory Comput.* **2005**, *1*, 1063−1078.
(31) Page, M.; McIver, J. W., Jr. *J. Chem. Phys.* **1988**, *88*, 922.
(32) Villà, J.; Truhlar, D. G. *Theor. Chem. Acc.* **1997**, *97*, 317−323.
(33) Alecu, I. M.; Zheng, J.; Zhao, Y.; Truhlar, D. G. *J. Chem. Theory Comput.* **2010**, *6*, 2872−2887.
(34) Fernandez-Ramos, A.; Ellingson, B. A.; Meana-Pañeda, R.; Marques, J. M. C.; Truhlar, D. G. *Theor. Chem. Acc.* **2007**, *118*, 813−826.
(35) Frisch, M. J.; Trucks, G. W.; Schlegel, H. B.; Scuseria, G. E.; Robb, M. A.; Cheeseman, J. R.; Scalmani, G.; Barone, V.; Mennucci, B.; Petersson, G. A.; Nakatsuji, H.; Caricato, M.; Li, X.; Hratchian, H. P.; Izmaylov, A. F.; Bloino, J.; Zheng, G.; Sonnenberg, J. L.; Hada, M.; Ehara, M.; Toyota, K.; Fukuda, R.; Hasegawa, J.; Ishida, M.; Nakajima, T.; Honda, Y.; Kitao, O.; Nakai, H.; Vreven, T.; Montgomery, Jr., J. A.; Peralta, J. E.; Ogliaro, F.; Bearpark, M.; Heyd, J. J.; Brothers, E.; Kudin, K. N.; Staroverov, V. N.; Kobayashi, R.; Normand, J.; Raghavachari, K.; Rendell, A.; Burant, J. C.; Iyengar, S. S.; Tomasi, J.; Cossi, M.; Rega, N.; Millam, N. J.; Klene, M.; Knox, J. E.; Cross, J. B.; Bakken, V.; Adamo, C.; Jaramillo, J.; Gomperts, R.; Stratmann, R. E.; Yazyev, O.; Austin, A. J.; Cammi, R.; Pomelli, C.; Ochterski, J. W.; Martin, R. L.; Morokuma, K.; Zakrzewski, V. G.; Voth, G. A.; Salvador, P.; Dannenberg, J. J.; Dapprich, S.; Daniels, A. D.; Farkas, Ö.; Foresman, J. B.; Ortiz, J. V.; Cioslowski, J.; Fox, D. J.; *Gaussian 09*, revision A.1; Gaussian, Inc.: Wallingford, CT, 2009.
(36) MOLPRO version 2009.1 is a package of ab initio programs written by: Werner, H.-J.; P. J. K., R. Lindh, Manby, F. R.; M. Schütz, Celani, P.; Korona, T.; Mitrushenkov, A.; Rauhut, G.; Adler, T. B.; Amos, R. D.; Bernhardsson, A.; Berning, A.; Cooper, D. L.; Deegan, M. J. O.; Dobbyn, A. J.; Eckert, F.; Goll, E.; Hampel, C.; Hetzer, G.; Hrenar, T.; Knizia, G.; C. Köppl, Liu, Y.; Lloyd, A. W.; Mata, R. A.; May, A. J.; McNicholas, S. J.; Meyer, W.; Mura, M. E.; Nicklass, A.; Palmieri, P.; K. Pflüger, Pitzer, R.; Reiher, M.; Schumann, U.; Stoll, H.; Stone, A. J.; Tarroni, R.; Thorsteinsson, T.; Wang, M.; Wolf, A. *MOLPRO*, version 2009.1.
(37) Zheng, J. Z., S.; Lynch, B. J.; Corchado, J. C.; Chuang, Y.-Y.; Fast, P. L.; Hu, W.-P.; Liu, Y.-P.; Lynch, G. C.; Nguyen, K. A.; Jackels, C. F.; Ramos, A. F.; Ellingson, B. A.; Melissas, V. S.; Villà, J.; Rossi, I.; Coitiño, E. L.; Pu, J.; Albu, T. V.; Steckler, R.; Garrett, B. C.; Isaacson, A. D.; Truhlar, D. G. *POLYRATE*, version 2010A; University of Minnesota: Minneapolis, 2010.
(38) Dauben, W. G.; Bridon, D. P.; Kowalczyk, B. A. *J. Org. Chem.* **1990**, *55*, 376−378.
(39) Dauben, W. G.; Kowalczyk, B. A.; Bridon, D. P. *Tetrahedron Lett.* **1989**, *30*, 2461−2464.
(40) Aveline, B. M.; Kochevar, I. E.; Redmond, R. W. *J. Am. Chem. Soc.* **1995**, *117*, 9699−9708.
(41) Frith, P. G.; McLauchlan, K. A. *J. Chem. Soc., Faraday Trans.* **1976**, *72*, 87−103.
(42) Newcomb, M.; Kaplan, J. *Tetrahedron Lett.* **1987**, *28*, 1615−1618.
(43) Barton, D. H. R.; Crich, D.; Motherwell, W. B. *Tetrahedron* **1985**, *41*, 3901−3924.
(44) Crich, D.; Quintero, L. *Chem. Rev.* **1989**, *89*, 1413−1432.
(45) Tuan, N. Q.; Gäumann, T. *Radiat. Phys. Chem.* **1977**, *10*, 263−273.
(46) Coote, M. L.; Lin, C. Y.; Zipse, H. In *Carbon-Centered Free Radicals and Radical Cations: Structure, Reactivity, and Dynamics*; Forbes, M. D. E., Ed.; John Wiley & Sons, Inc.: Hoboken, NJ, 2010; Vol. *3*, pp 83−104.
(47) Roberts, B. P. *Chem. Soc. Rev.* **1999**, *28*, 25−35.
(48) Roberts, B. P. *J. Chem. Soc., Perkin Trans. 2* **1996**, 2719−2725.
(49) Roberts, B. P.; Steel, A. J. *J. Chem. Soc., Perkin Trans. 2* **1994**, 2155−2162.
(50) Pross, A.; Yamataka, H.; Nagase, S. *J. Phys. Org. Chem.* **1991**, *4*, 135−140.
(51) Pross, A. *Adv. Phys. Org. Chem.* **1985**, *21*, 99−196.
(52) Pross, A.; Shaik, S. S. *Acc. Chem. Res.* **1983**, *16*, 363−370.
(53) Shaik, S. S. *Prog. Phys. Org. Chem.* **1985**, *15*, 197−337.
(54) Pross, A. *Theoretical and Physical Principles of Organic Reactivity*; John Wiley & Sons: New York, 1995.

(55) *NIST Chemistry WebBook, NIST Standard Reference Database Number 69*; Linstrom, P. J., Mallard, W. G., Eds.; National Institute of Standards and Technology: Gaithersburg, MD, 20899, http://webbook.nist.gov (retrieved June 12, 2012).
(56) Shaik, S.; Danovich, D.; Silvi, B.; Lauvergnat, D.; Hiberty, P. C. *Chem.—Eur. J.* **2005**, *11*, 6358−6371.
(57) Shaik, S.; Maitre, P.; Sini, G.; Hiberty, P. C. *J. Am. Chem. Soc.* **1992**, *114*, 7861−7866.
(58) Shaik, S. S.; Danovich, D.; Wu, W.; Hiberty, P. C. *Nat. Chem.* **2009**, *1*, 443−449.
(59) Coote, M. L.; Pross, A.; Radom, L. *Org. Lett.* **2003**, *5*, 4689−4692.
(60) Izgorodina, E. I.; Coote, M. L.; Radom, L. *J. Phys. Chem. A* **2005**, *109*, 7558−7566.
(61) Lin, C. Y.; Peh, J.; Coote, M. L. *J. Org. Chem.* **2011**, *76*, 1715−1726.
(62) Hiberty, P. C.; Megret, C.; Song, L.; Wu, W.; Shaik, S. *J. Am. Chem. Soc.* **2006**, *128*, 2836−2843.
(63) See for example: (a) Pu, J. G., J.; Truhlar, D. G. *Chem. Rev.* **2006**, *106*, 3140. (b) Truhlar, D. G. *J. Phys. Org. Chem.* **2010**, *23*, 660. (c) Ley, D.; Gerbig, D.; Schreiner, P. R. *Org. Biomol. Chem.* **2012**, *10*, 3781. (d) Schreiner, P. R.; Reisenauer, H. P.; Ley, D.; Gerbig, D.; Wu, C.-H.; Allen, W. D. *Science* **2011**, *332*, 1300. (e) Shelton, G. R.; Hrovat, D. A.; Borden, W. T. *J. Am. Chem. Soc.* **2007**, *129*, 164.
(64) Engel, P. S.; Chae, W.-K.; Baughman, S. A.; Marschke, G. E.; Lewis, E. S.; Timberlake, J. W.; Luedtke, A. E. *J. Am. Chem. Soc.* **1983**, *105*, 5030−5034.
(65) Lomas, J. S.; Fain, D.; Briand, S. *J. Org. Chem.* **1990**, *55*, 1052−1058.
(66) Lomas, J. S.; Briand, S. *Tetrahedron Lett.* **1989**, *30*, 707−710.
(67) Alhambra, C.; Gao, J.; Corchado, J. C.; Villa, J.; Truhlar, D. G. *J. Am. Chem. Soc.* **1999**, *121*, 2253−2258.
(68) Cui, Q.; Karplus, M. *J. Am. Chem. Soc.* **2002**, *124*, 3093−3124.
(69) Truong, T. N.; McCammon, A. J. *J. Am. Chem. Soc.* **1991**, *113*, 7504−7508.
(70) Storer, J. W.; Houk, K. N. *J. Am. Chem. Soc.* **1993**, *115*, 10426−10427.
(71) Corchado, J. C.; Espinosa-Garcia, J. *J. Chem. Phys.* **1996**, *105*, 3160−3167.
(72) Villa, J.; Gonzalez-Lafont, A.; Lluch, J. M. *J. Phys. Chem.* **1996**, *100*, 19389−19397.